Nanotechnology **20** (2009) 355201 (5pp) doi:10.1088/0957-4484/20/35/355201

Minority carrier effects in nanoscale Schottky contacts

Lifeng Hao[1] **and P A Bennett**[1,2]

[1] School of Materials, Arizona State University, Tempe, AZ 85287, USA
[2] Department of Physics, Arizona State University, USA

Received 10 June 2009, in final form 5 July 2009
Published 11 August 2009
Online at stacks.iop.org/Nano/20/355201

Abstract

We report the current–voltage behavior for nanoscale point contacts to Si(111) obtained in ultrahigh vacuum using scanning tunneling microscopy. Epitaxial $CoSi_2$ islands provide single-crystal contacts with well-defined size and shape. The zero bias conductance is found to be independent of the island size (10^2–10^4 nm^2) and shape, but varies strongly with the surface Fermi level position. This behavior is explained by the recombination–generation current from minority carriers at the free surface, which may be orders of magnitude larger than the majority carrier thermionic or tunnel currents across the contact interface. This can give rise to large shifts of the apparent ideality factor and Schottky barrier height for the point contact.

(Some figures in this article are in colour only in the electronic version)

As electronic devices shrink to the nanoscale, the role of electrical contacts becomes increasingly important. Indeed, the contacts become an intrinsic part of the functional unit, and can dominate the device operation [1, 2]. Some devices, such as nanowire transistors rely explicitly on contact effects rather than channel effects to control current flow [3].

Point contacts date from 1874, and provided the first solid state rectifiers, free from interface oxide effects [4]. Point contacts remain important today, since they can operate at very high frequency, and with very high sensitivity [5]. They may also be utilized in large arrays for efficient solar cell devices [6]. The geometry of the point contact creates an intense electric field that gives rise to strong tunneling and associated 'leakage' effects. Such effects may arise in multicomponent nanoelectronic structures, where they are difficult to control or even to identify. In this sense, the point contact is a prototype structure that allows the study of such effects in a controlled manner.

The current–voltage (I–V) behavior for an ideal Schottky diode may be written as

$$I(V) = AA^*T^2 \exp\left(-\frac{q\Phi_{SB}}{kT}\right)\left[\exp\left(\frac{qV}{nkT}\right) - 1\right], \quad (1)$$

where A^*, n and Φ_{SB} are the Richardson constant, the effective 'ideality factor' and Schottky barrier height, respectively [7]. Several groups have investigated the I–V behavior of metal–semiconductor point contacts, and have reported anomalous values for n and Φ_{SB} obtained by fitting the data to equation (1). This behavior has been variously attributed to tunneling or to ohmic conduction through surface states or to screening by a strongly pinned surface Fermi level adjacent to the contact [8–12].

In this paper, we report *in situ* I–V measurements of nanometer-sized metal contacts to a Si(111) substrate using UHV-STM. Epitaxial $CoSi_2$ islands provide well-defined contacts with variable size in the range of 10^2–10^4 nm^2. We find that the conductance near zero bias, G_0, is large and independent of contact size or Schottky barrier height, while the I–V curves show large and voltage-dependent ideality factors 'n', in accord with similar earlier measurements [8–12]. Furthermore, G_0 is found to vary strongly with temperature and with surface Fermi level position, which is adjusted by submonolayer coverages of Co. This behavior is explained by a surface recombination–generation (RG) current of minority carriers at the surrounding free surface. This current is much larger than the majority carrier current across the metal–semiconductor interface itself. This mechanism, which appears only for nanometer-sized contacts, has not been considered in earlier point contact work, and provides a physical origin for anomalous n, Φ_{SB} values that have been widely observed. It also provides new insight into surface conductivity measurements using nanoprobes. This effect may arise for any small metallic feature in contact with a semiconductor surface or interface.

All experiments were performed in a UHV system with base pressure of 1×10^{-10} Torr. Si(111) substrates (n-type,

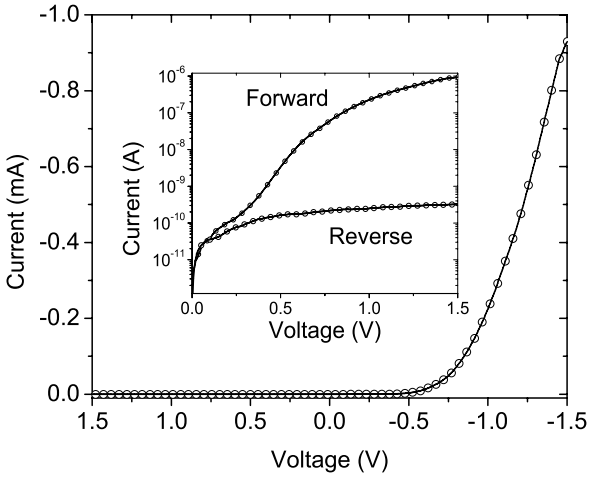

Figure 1. A full I–V curve for a 420 nm^2 $CoSi_2$ island. Inset shows the same curve in a semilog plot.

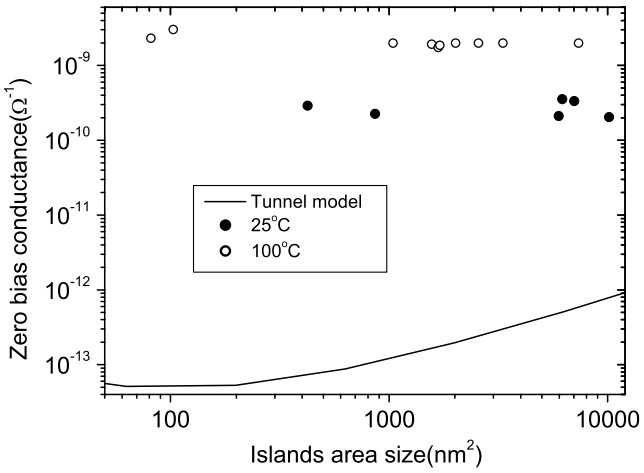

Figure 2. Zero bias conductance as a function of island size at $T = 25$ and 100 °C. Solid line is calculated tunnel current for a spherical barrier model.

$\rho \sim 1\ \Omega$ cm) were degassed at 600 °C for 12 h followed by repeated brief heating to 1200 °C and slow cooling to yield a clean 7 × 7 surface. Epitaxial single-crystal $CoSi_2$ islands were grown by depositing 0.4 monolayer (ML) Co and annealing at 600 °C for 5 min. Different-shaped islands (triangle, hexagonal) with size ranging from 10^2 to 10^4 nm^2 were obtained in a single growth cycle with identical surface condition [13]. For some experiments, the surface Fermi level was adjusted by depositing Co at 650 °C, which produces a 1 × 1 structure with saturation coverage of 1/7 ML [14, 15]. The surface Fermi level is assumed linear with coverage from 0.65 eV at 0 ML to 0.42 eV at saturation [16, 17]. The STM tips were electrochemically etched tungsten. Electrical contact with the surface was made by first bringing the tip into tunnel position, then pressing forward 1 nm. This procedure allowed reproducible electrical measurements while retaining step-resolved imaging. Sample temperature was measured by optical pyrometer for $T > 650$ °C or by thermocouple for $T < 700$ °C, with an accuracy of 50 °C.

A typical I–V curve is shown in figure 1 for a 420 nm^2 island. This curve shows rectifying behavior, and may be characterized by a model of a Schottky Barrier (described by equation (1)) plus parallel resistor, with $R_\parallel = 4 \times 10^9\ \Omega$, $n = 2$–3 and $\Phi_{SB} = 0.42$ V (ideal values are $R_\parallel = \infty$, $n = 1$ and $\Phi_{SB} = 0.67$ V [18]). $R_\parallel$ is much smaller than the resistance of the Schottky diode, indicating a large leakage current. The I–V curves for a whole set of islands with size ranging from 10^2 to 10^4 nm^2 are similar in shape and magnitude. For ease of reference in the reminder of his paper, we will characterize these curves by their zero bias conductivity, G_0, obtained from the slope of the I–V curve in the range ±0.05 V. We find that G_0 is independent of island size and shape, with a constant value of $G_0 \sim 2.5 \times 10^{-10}\ \Omega^{-1}$ at 25 °C and $G_0 \sim 2 \times 10^{-9}\ \Omega^{-1}$ at 100 °C, as shown in figure 2. Data from Smit *et al* for the same $CoSi_2$/Si(111) system show a similar constant value of $G_0 \sim 1 \times 10^{-10}\ \Omega^{-1}$ at 25 °C, for low-doped samples (inset to figure 1 in [19]). This current cannot be due to thermionic emission, which would yield $G_0 \sim 2 \times 10^{-14}\ \Omega^{-1}$ for an island size of 10^3 nm^2

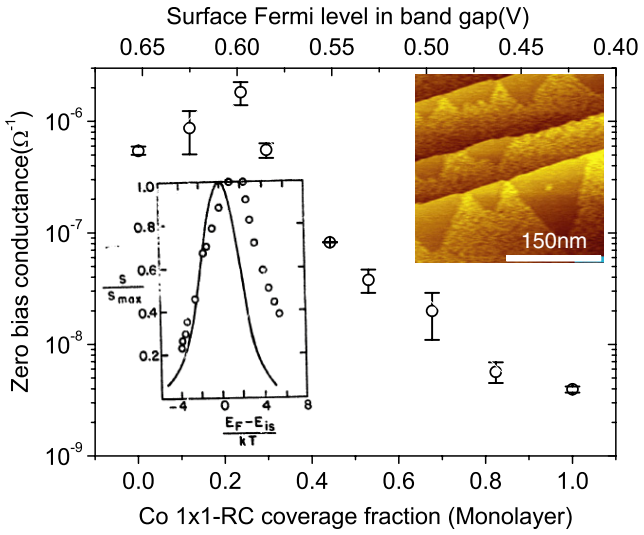

Figure 3. Zero bias conductance as a function of Co-1 × 1 fractional coverage θ. The right inset is the STM image (1.5 V bias, 1 nA) for $\theta = 0.6$. The left inset shows the normalized surface recombination velocity as a function of surface Fermi level position for Ge(111). The circles shows the experimental data, and the solid curve is the calculated result (after [20]).

and $\Phi_{SB} = 0.67$ eV at 25 °C. This current cannot be due to tunneling either, since that contribution is far too small. This may be directly calculated for a spherical contact embedded in bulk silicon, and is shown in the figure. Finally, G_0 cannot be due to ohmic surface conductance, since that would be independent of T, unlike the measurement.

The discussion above suggests that the point contact conductance is dominated by an additional (parallel) non-ohmic component. To explore this hypothesis, the surface was altered by adding a submonolayer of Co atoms at 650 °C, changing the reconstruction from 7 × 7 to 1 × 1, and also shifting the surface Fermi level from 0.65 to 0.42 eV, as indicated on the top axis of figure 3. Here θ is the fraction of saturation coverage of 1/7 ML. The inset shows an STM

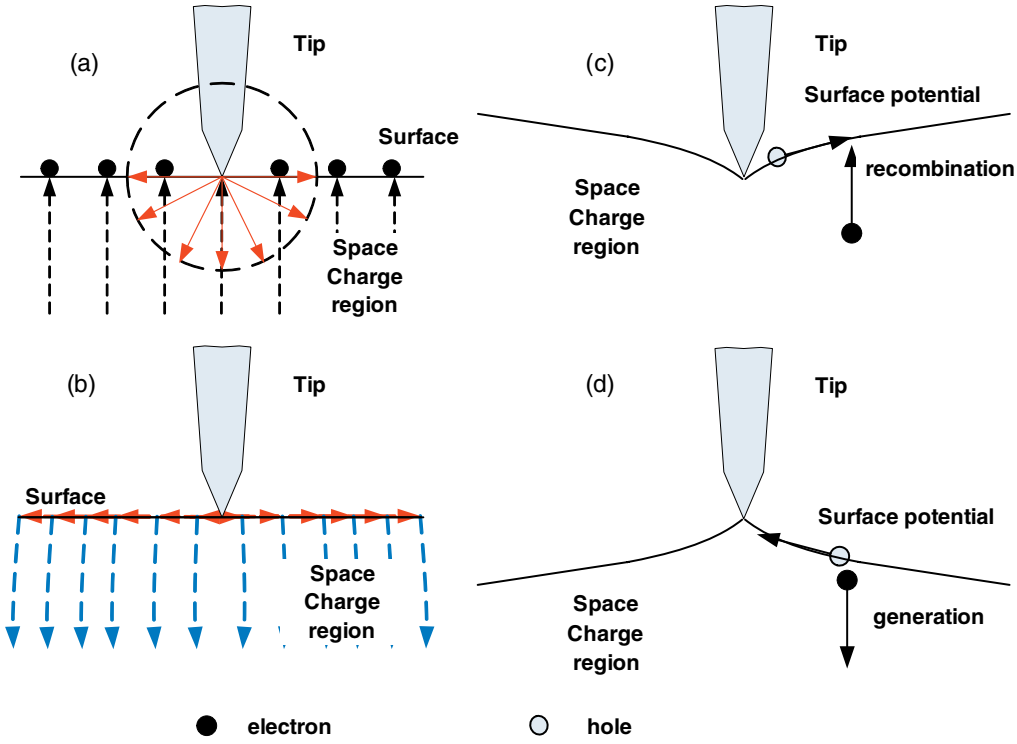

Figure 4. (a) Schematic potential distribution for point contact on free surface. Broken arrows indicate electric field in the space charge region due to charged surface states (n-type), solid arrows indicate electric field due to tip (forward) bias. (b) Current flow of majority (broken) and minority (solid) arrows under forward bias. Surface potential and carrier motion under forward (c) and reverse (d) bias.

image at $\theta = 0.6$, with clear 1×1 (light) and 7×7 regions (dark). For these variable coverage experiments, the STM tip itself was used for the point contact with an estimated area of 10^2 nm^2. (As shown above, G_0 is insensitive to the size of the contact). The I–V curves showed no variation between 7×7 and 1×1 regions, with a scatter for multiple measurements as shown by the error bars. The variation of G_0 with Co coverage (and associated surface Fermi level) is striking: it begins at $G_0 = 6 \times 10^{-7}\ \Omega^{-1}$ for clean 7×7, rises to a maximum of $2 \times 10^{-6}\ \Omega^{-1}$ at $\theta = 0.2$, then decreases to $4 \times 10^{-9}\ \Omega^{-1}$ at $\theta = 1.0$. Hasegawa *et al* report similar values for a W or Al STM tip on clean Si(111)-7×7 for both n-type and p-type substrates [21]. This indicates that the total current near zero bias is insensitive to the electronic and geometric structure of the contact.

The strong, non-monotonic variation of G_0 with Co coverage cannot be explained by the conduction through the near-surface space–charge layer, which depends on band bending and surface Fermi level, but in a monotonic way [22]. We propose instead that this behavior is due to a large R–G current of minority carriers flowing through the free surface that surrounds the point contact. Surface R–G events are characterized by the surface recombination velocity, s, which may be written as [20],

$$s = \sigma_s v_{\rm th}(kT D_{\rm st}) \left\{ \frac{\cosh^{-1}\left(\frac{p_s+n_s}{2n_i}\right)}{\left[\left(\frac{p_s+n_s}{2n_i}\right)^2 - 1\right]^{1/2}} \right\} \frac{N_A}{n_i}, \qquad (2)$$

where σ_s is the capture cross section for both electrons and holes, $v_{\rm th}$ is the thermal velocity, n_i is the intrinsic carrier concentration, $D_{\rm st}$ is the density per unit area and energy for the surface recombination centers, N_A is the doping concentration and n_s (or p_s) is the electron (or hole) density at the surface. For zero bias condition, we have $n_s = n_i \exp[(E_{Fs} - E_i)/kT]$ and $p_s = n_i \exp[-(E_{Fs} - E_i)/kT]$ in which E_{Fs} is the surface Fermi level and E_i is the intrinsic Fermi level. We note that s depends on $D_{\rm st}$ linearly and on E_{Fs} in a complicated way. Actually, equation (2) shows that s varies exponentially with E_{Fs}, being sharply peaked near E_i (near mid-gap), as illustrated in the inset of figure 3. The measured current clearly follows this general trend. This indicates that E_{Fs}, instead of $D_{\rm st}$, dominates the variation of s and G_0, although $D_{\rm st}$ might be changed with Co coverage as well.

The current flow pattern for a point contact on a free surface is shown in schematic form in figure 4. Under equilibrium conditions, with zero applied bias, charged surface states pin the Fermi level and create a gradual variation of conduction band edge versus depth (band bending). An external bias voltage applied to the tip creates an approximately radial electric field which acts as the driving force for net current flow. This field drives a thermionic current (majority carriers excited over the Schottky barrier) as well as a tunneling current (majority carriers tunneling through the barrier). These currents are small compared with the total observed current, as discussed above. The R–G current arises because the tip-induced voltage shifts the carrier density out of thermal equilibrium ($np \neq n_i^2$). This causes generation or recombination processes which take place mostly on the free surface surrounding the tip.

For example, under reverse bias (tip negative, for n-type Si), the potential of the free surface near the tip is raised, causing $n_s p_s < n_i^2$, which in turn causes thermal generation of electron–hole pairs at recombination centers on the free surface. The generated electrons are swept out of the depletion region and into the bulk by the built-in field, while the generated holes go to the tip, driven by drift and diffusion forces. Under forward bias, the same process occurs in reverse: holes are injected from the tip into the surface states directly or into the surface space charge region, move across the surface and recombine there with electrons that arrive from the bulk. It should be noted that the built-in field holds minority carriers near the surface everywhere. The total R–G current then involves a series sum of minority current along the surface and majority current to/from the bulk, connected via the surface R–G processes.

The magnitude of current flow depends primarily on the degree of departure from equilibrium (separation of quasi-Fermi levels, which varies with distance from the tip) and the efficiency of the R–G process. Indeed, following Fitzgerald [20], the surface generation current for a fully depleted surface may be roughly estimated as

$$I_g = qsn_iA, \tag{3}$$

where A is the collection area. For the Si(111)-7 × 7 surface, we use $s \sim 2 \times 10^6$ cm s^{-1} [23], and $A \sim (100\ \mu\text{m})^2$ [24]. A is large, since it is determined by the minority carrier diffusion length for Si which can be 100 μm. This geometry is similar to the gate-controlled diode configuration, in which surface generation current is collected from areas of this size [20]. Thus, the estimated surface generation current is 0.3 μA, which is close to the measured reverse bias current (0.5 μA) for direct W tip contact to clean 7 × 7 surface. The above simple estimate suffices to verify the dominance of surface R–G current over interface current for small contacts. A full calculation of the I–V behavior would have to include the variation of surface potential, carrier density and current flow.

The observed independence of G_0 on contact size, as shown in figure 2, can be easily understood since, for a small contact, the total current is dominated by the surface R–G current which is not related to the contact. For large contacts, however, the thermionic and/or tunneling current will exceed the surface current, since they scale with island size. For our substrate, this occurs for island size $r > 1$ μm. This cross-over size will depend on doping level and surface recombination rate. Finally, we note that the R–G current increases rapidly with temperature since $n_i \sim \exp(-E_g/2kT)$, in accord with the data.

The dominance of minority current (via surface R–G process) for nanoscale Schottky contacts is in striking contrast to planar Schottky contacts. In a planar Schottky contact, the majority and minority currents are closely coupled, with the minority current generally negligible in relative size [7]. For the nanoscale Schottky point contact, however, these currents are decoupled: the majority current flows across the interface while the minority current may flow along the free surface. As a result, the minority current may strongly dominate if the surface is electrically active.

The surface R–G current will be present for any biased metallic contact on a semiconductor surface. In practical devices, the contact geometry is carefully designed to reduce R–G currents and other 'leakage' effects [7]. This requires careful control of the surface recombination velocity 's'. For Si/SiO$_2$, one can have $s < 1$ cm s^{-1}, which would bring G_0 into an acceptable range of 10^{-10} Ω^{-1} [24, 25]. For multicomponent and/or prototype nanoelectronic structures, however, s is not well known or controlled, and may be very large.

Surface R–G effects may also be important in electrical nanoprobe measurements, such as 'scanning spreading resistance', which is widely used to measure substrate conductivity [26, 27], or multi-tip STM, which is used to measure conductance of surface layers. The surface R–G currents can significantly alter the potential distribution and current flow, and must be included in a proper model of the probe. This has not been done, to date, which may explain the orders of magnitude variation in the reported conductance for intrinsic surface states on clean silicon [28–31].

In summary, we have shown that the current flow for nanoscale Schottky contacts on Si(111) is strongly dominated by minority carrier recombination–generation current at the free surface. This current will occur for any small metal contact to a semiconductor surface and can be magnitudes larger than the majority carrier thermionic or tunnel currents across the metal–semiconductor interface. This may be misinterpreted as large shifts of the apparent ideality factor, Schottky barrier height or spreading resistance for small contacts and may also perturb multi-probe surface conductivity measurements.

Acknowledgments

This work was supported by NSF grant DMR0503705.

References

[1] Lin Y F and Jian W B 2008 *Nano Lett.* **8** 3146
[2] Chen Z H, Appenzeller J, Knoch J, Lin Y M and Avouris P 2005 *Nano Lett.* **5** 1497
[3] Heinze S, Tersoff J, Martel R, Derycke V, Appenzeller J and Avouris P 2002 *Phys. Rev. Lett.* **89** 106801
[4] Braun F 1874 *Ann. Phys. Chem.* **153** 556
[5] Zhu S Y, Lo G Q, Yu M B and Kwong D L 2008 *Appl. Phys. Lett.* **93** 073503
[6] Kotsovos K and Misiakos K 2001 *J. Appl. Phys.* **89** 2491
[7] SZE S M and NG K K 2006 *Physics of Semiconductor Devices* (Hoboken, NJ: Wiley)
[8] Hasegawa H, Sato T and Kaneshiro C 1999 *J. Vac. Sci. Technol.* B **17** 1856
[9] Oh J and Nemanich R J 2002 *J. Appl. Phys.* **92** 3326
[10] Park W I, Yi G C, Kim J W and Park S M 2003 *Appl. Phys. Lett.* **82** 4358
[11] Kubo O, Shingaya Y, Aono M and Nakayama T 2006 *Appl. Phys. Lett.* **88** 233117
[12] Soubiron T, Stiufiuc R, Patout L, Deresmes D, Grandidier B, Stievenard D, Koble J and Maier M 2007 *Appl. Phys. Lett.* **90** 102112
[13] Ross F M, Bennett P A, Tromp R M, Tersoff J and Reuter M 1999 *Micron* **30** 21
[14] Bennett P A, Copel M, Cahill D, Falta J and Tromp R 1992 *Phys. Rev. Lett.* **69** 1224

[15] Bennett P A, Parikh S, Lee M and Cahill D 1994 *Surf. Sci.* **312** 377
[16] Himpsel F J, Hollinger G and Pollak R A 1983 *Phys. Rev.* B **28** 7014
[17] Flammini R, Wiame F, Belkhou R and Taleb-Ibrahimi A 2004 *Appl. Surf. Sci.* **233** 411
[18] Brillson L 1982 *Surf. Sci. Rep.* **2** 123
[19] Smit G D J, Rogge S, Caro J and Klapwijk T M 2004 *Phys. Rev.* B **69** 035338
[20] Fitzgerald D J and Grove A S 1968 *Surf. Sci.* **9** 347
[21] Hasegawa Y, Lyo I W and Avouris P 1996 *Surf. Sci.* **358** 32
[22] Hasegawa S, Tong X, Takeda S, Sato N and Nagao T 1999 *Prog. Surf. Sci.* **60** 89
[23] Hsu J, Bahr C, Felde A, Downey S, Higashi G and Cardillo M 1992 *J. Vac. Sci. Technol.* A **10** 985
[24] Aspnes D E 1983 *Surf. Sci.* **132** 406
[25] Kerr M J and Cuevas A 2002 *Semicond. Sci. Technol.* **17** 35
[26] De Wolf P, Stephenson R, Trenkler T, Clarysse T, Hantschel T and Vandevorst W 2000 *J. Vac. Sci. Technol.* B **18** 361
[27] Eyben P, Denis S, Clarysse T and Vandervorst W 2003 *Mater. Sci. Eng.* B **102** 132
[28] Tanikawa T, Yoo K, Matsuda I, Hasegawa S and Hasegawa Y 2003 *Phys. Rev.* B **68** 113303
[29] Yoo K and Weitering H 2002 *Phys. Rev.* B **65** 115424
[30] Wells J W, Kallehauge J F, Hansen T M and Hofmann P 2006 *Phys. Rev. Lett.* **97** 206803
[31] Heike S, Watanabe S, Wada Y and Hashizume T 1998 *Phys. Rev. Lett.* **81** 890